Rheologica Acta Rheol Acta 33:307–316 (1994)

Microstructure and melt flow behavior of a starch-based polymer

C. Bastioli, V. Bellotti, and A. Rallis

Novamont spa (Montedison Group), Novara, Italy

Abstract: Results on some physical properties and on melt processing of a starch-based polymer under steady-state shearing are presented. A peculiar microstructure involving a strong pseudoplastic behavior at high shear rates as well as yield stress at lower ones is discussed. A model is proposed to explain the characteristic viscoelastic behavior of this material based on hydrophylic and hydrophobic interactions between starch and vinyl-alcohol copolymers.

In spite of the highly structured and composite nature of this class of materials, the full body of results reveals that they can be easily processed by means of common manufacturing techniques involving melt pumping and die forming. A comparison with a low density polyethylene (LDPE) grade for film blowing is also shown.

Key words: Maize starch – biodegradable polymer – melt rheology – yield stress – die-swell

Introduction

The increasing problem of solid waste managment, particularly of plastics, and the increased sensitivity for the environmental problems have strongly oriented the research activity towards new materials based on renewable sources, and mainly on starch.

Their rheological behavior up to now was not extensively studied (Ryle, 1991; Bastioli et al., 1991a). Unusual properties however can be forecast on the basis of their composite nature, and are able to generate a wide variety of morphologies.

In order to understand viscoelastic properties and morphology of these materials, the shear flow analysis of a commercial Mater-Bi® grade for film blowing, manufactured by Novamont, was performed in comparison with a low density polyethylene (LDPE).

Experimental and results

Mater-Bi® AF05H grade contains about 60% of maize starch and natural additives and 40% of ethylene-vinyl alcohol copolymer 40/60 (mol/mol) (Bastioli et al., 1993a). Its physical properties and melt flow rate data according to ASTM-D 1238 are reported in Table 1 and Fig. 1 respectively.

Commercial pellets of AF05H were used without any additional treatment (i.e., drying, etc.). An LDPE grade for film-blowing, Riblene CF2313 (MFI = 2, $M_W = 144000$, $M_W/M_N = 7$), manufactured by EniChem, was also tested as a comparison.

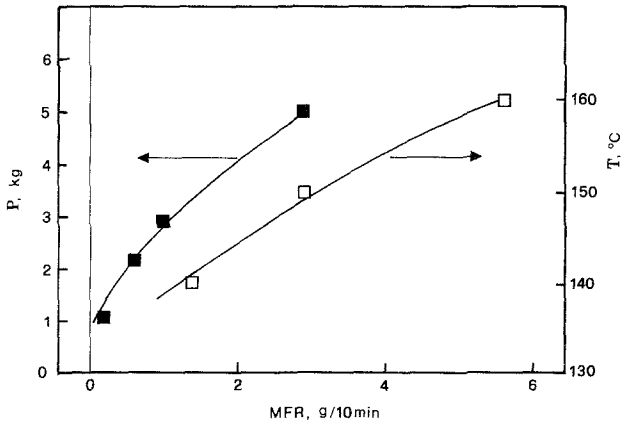

Fig. 1. Melt flow rate of AF05H (test method: ASTM-D1238); ■: vs. weight P ($T = 150\,°C$) and □: vs. temperature T ($P = 5$ kg)

Table 1. Physical properties of Mater-Bi® AF05H

Specific weight (ASTM-D1505)	g/cm^3	1.26
Melting point (peak)	°C	135
Glass transition temperature	°C	53
Specific heat (at 117 °C)	Kj/kg °C	2.74
Linear expansion coefficient	°C g	1.33×10^{-6}
Moisture content (Karl-Fischer)*	%	2.75

* Before titration, the polymer was dissolved in DMSO at 80 °C in a closed container.

Flow properties

Different viscometric equipment, described in Table 2, were employed to study the flow behavior of AF05H. The analysis was performed mainly at $T = 140$ and 150 °C; additional data carried out at 160 °C were used for determining the flow activation energy.

The slit-die viscometer was instrumented with three melt thermocouples and pressure transducers, regularly spaced, whose range was $0 \div 20$, $0 \div 35$, and $0 \div 50$ MPa, respectively. The pressure transducers were set flush (within 0.03 mm) into the fully developed flow zone of the slit channel; the closest transducer to the slit entry was $60 \cdot H$ far from it (H: slit height). The temperature along the slit was kept constant within 1 °C during the experimental runs. Figure 2 reports a schematic diagram of the slit die viscometer (SDV) employed in this work.

For the SDV, the wall shear stress τ was determined by the longitudinal pressure gradient dP/dL (Fig. 2),

$$\tau = \frac{H}{2}\frac{dP}{dL} \tag{1}$$

and the wall shear rate Γ through equation:

$$\Gamma = \frac{6Q}{WH^2}\left[\frac{2n+1}{3n}\right] \tag{2}$$

For the capillary systems CAP1 and CAP2, τ and Γ are given respectively by,

$$\tau = \frac{\delta P}{2(\varepsilon + L/R)} \tag{3}$$

$$\Gamma = \frac{4Q}{\pi R^3}\left[\frac{3n+1}{4n}\right] \tag{4}$$

where: Q = vol. flow rate, W = slit width, H = slit height, $n = d\ln\tau/d\ln\Gamma_{app}$, ε = end correction (Bagley, 1957), δP = overall capillary pressure drop, L = capillary length, R = capillary radius. The terms between square brackets in Eqs. (2) and (4) take into account the non-parabolic velocity profile across capillary channels. For CAP2 the true wall shear stress was evaluated with the help of three capillaries, having $D = 1.27$ mm and L/D ratio 15, 20, and 30, respectively, thus determining the fictitious length extensions $\varepsilon \cdot R$ (Bagley plots). For CAP 1 the end effects were neglected ($\varepsilon = 0$).

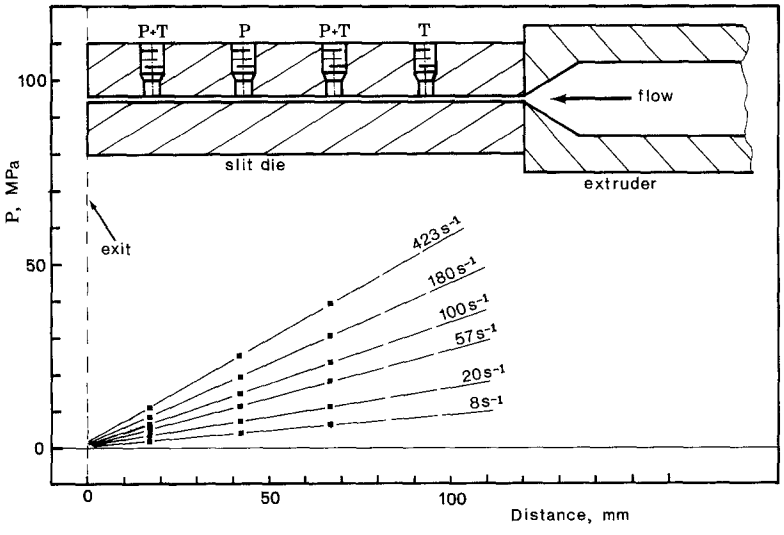

Fig. 2. Schematic diagram of the slit-die viscometer (SDV). Plots are longitudinal pressure profiles of AF05H at different shear rates ($T = 140$ °C)

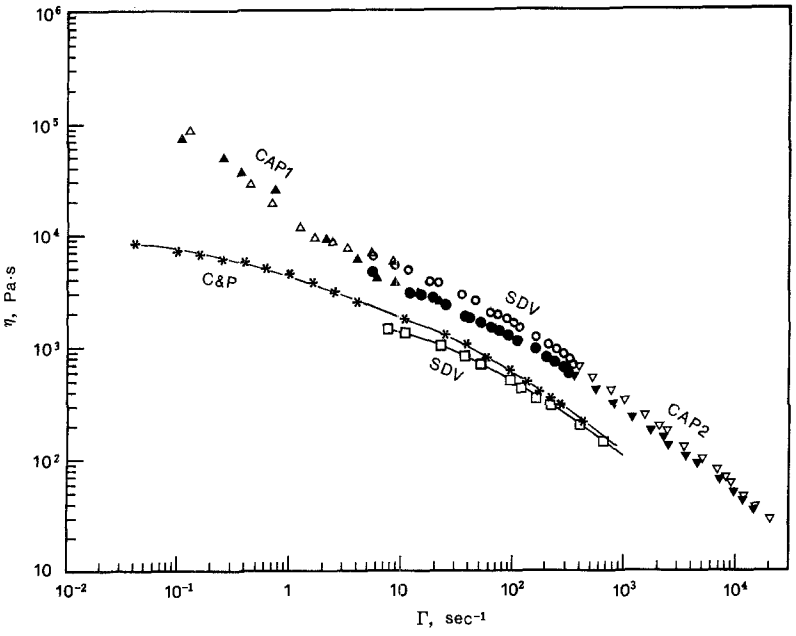

Fig. 3. Shear viscosity curves carried out with different viscometric systems (see Table 2). a) AF05H: $T = 140\,°C$ (open symbols), $T = 150\,°C$ (closed symbols); b) LDPE: ∗ = 180 °C, □ = 200 °C

Low density polyethylene was tested by a slit-die viscometer at 180° and 200 °C and by a cone-and-plate Instron 3250 rheogoniometer, at 180 °C, in steady-state conditions. The recorded net axial thrust F between cone and plate allowed one to estimate the first normal stress difference for polyethylene:

$$N_{11}|_{C\&P} = 2F/(\pi \cdot R^2) \quad \text{where } R\text{: cone radius} \qquad (5)$$

Log-log plots of shear viscosity versus shear rate obtained by means of the different viscometric systems are reported in Fig. 3 for both polymers.

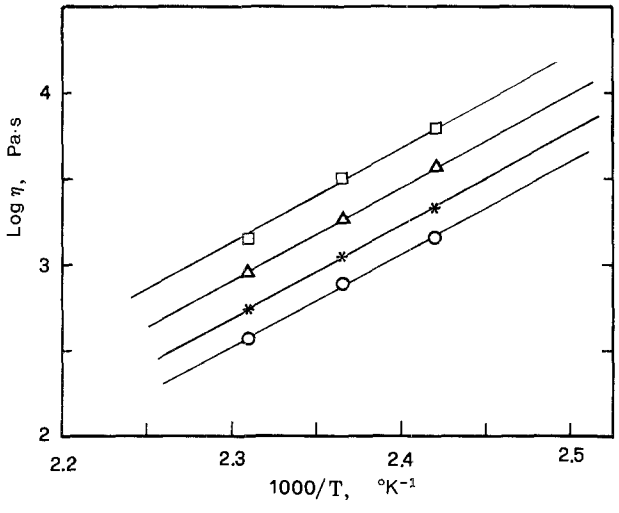

Fig. 4. Arrhenius plots of AF05H at constant shear stress. □ = 35 kPa; △ = 75 kPa; ∗ = 125 kPa; ○ = 170 kPa

The effect of temperature on AF05H shear viscosity is shown in Fig. 4 at different shear stress levels.

Figure 5 shows flow curves as well as the first normal stress difference N_{11} of AF05H versus shear rate Γ; N_{11} data for both polymers were obtained from exit pressure values (Han, 1976):

$$N_{11}|_{ex} = P_{ex} + \tau \cdot (dP_{ex}/d\tau) \,, \qquad (6)$$

where P_{ex} = exit pressure. The P_{ex} was extrapolated from pressure readings along the slit die (Fig. 2).

Plots of P_{ex} versus wall shear stress and of first normal stress difference ($N_{11}|_{ex}$ and $N_{11}|_{C\&P}$) versus wall shear rate are reported in Figs. 6 and 7 respectively.

Die-swell

The swelling ratio B (extrudate diameter d to capillary diameter D) was estimated by means of two experimental techniques:

a) Frozen die-swell: The extrudate was frozen by immersion in cold water, 30 mm far from CAP 3 exit, and dried by moisture-free air. The diameter was then measured by a micrometer.

b) Photographic die-swell: The extrudate was photographed in steady-state conditions, 3D/4 far from CAP 3 exit (scheme as in Fig. 8). All photographs were taken in non-isothermal conditions, when the

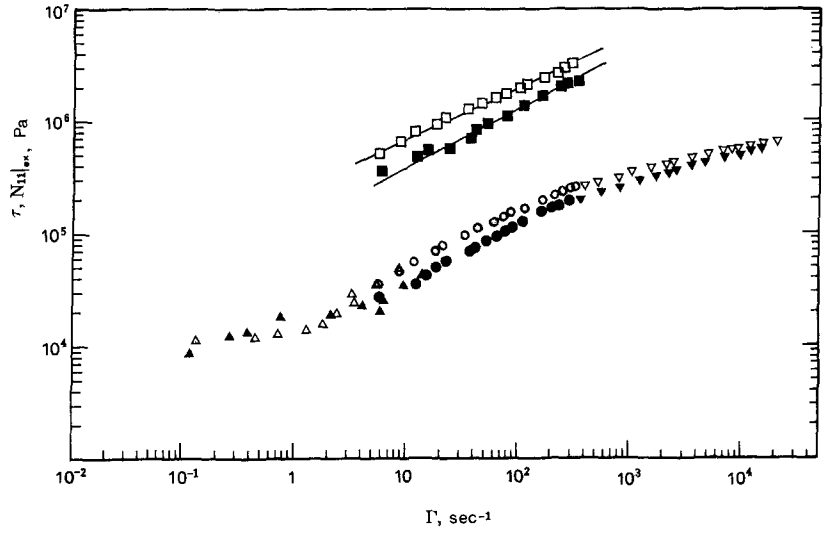

Fig. 5. AF05H: a) Flow curves of AF05H at 140° and 150 °C (symbols as in Fig. 3); b) normal stress difference $N_{11}|_{ex}$ vs. wall shear rate: □ = 140 °C, ■ = 150 °C

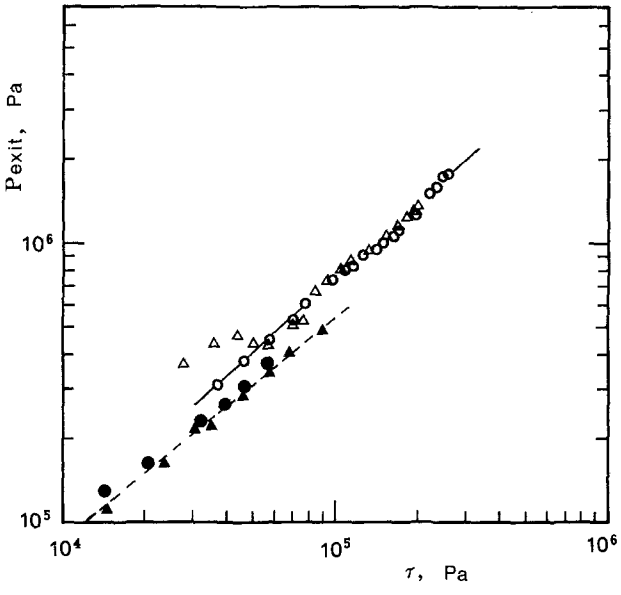

Fig. 6. Exit pressure vs. wall shear stress. a) AF05H: ○ = 140 °C, △ = 150 °C; b) LDPE: ● = 180 °C, ▲ = 200 °C

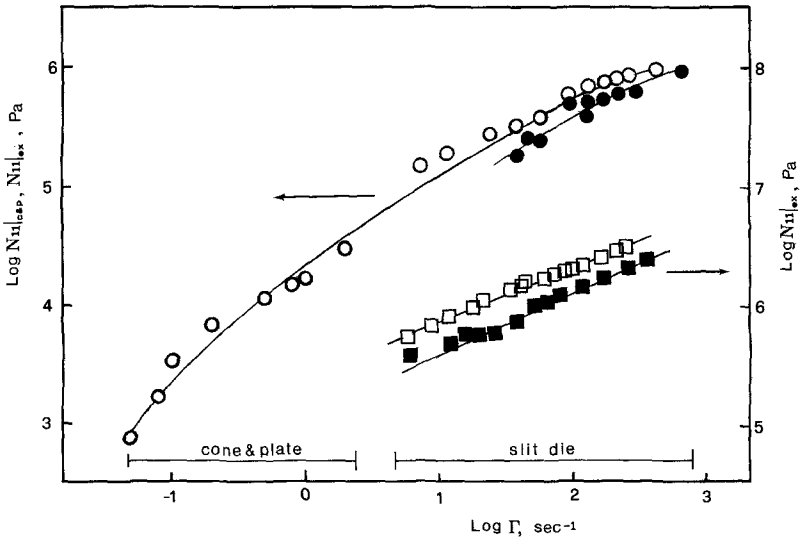

Fig. 7. Normal stress difference vs. shear rate at different temperatures and test equipments (see Table 2). a) LDPE (left axis): ○ = 180 °C, ● = 200 °C; b) AF05H (right axis): □ = 140 °C, ■ = 150 °C

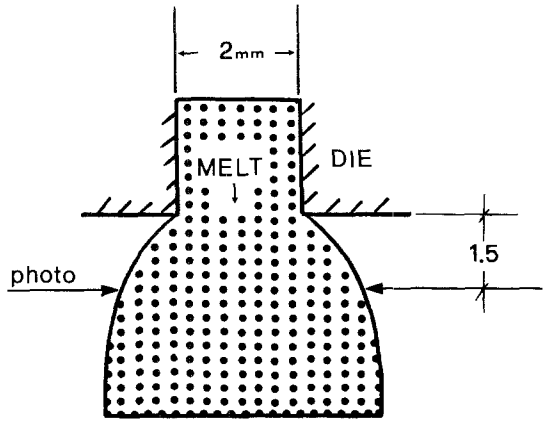

Fig. 8. Scheme of the photographic die-swell procedure employed in this work

same amount of melt ($\simeq 1.5$ gr) was extruded from the capillary outlet.

The experimental die-swell results are plotted in Fig. 9 against apparent shear rate, Γ_{app}. Higher die-swell ratios were measured by means of technique (a), this is in relation to the different distance from the die exit.

Surface instability of AF05H: A typical surface roughness was observed at wall shear rates lower than a critical value Γ_{cr}, increasing with temperature. Critical conditions become temperature independent when expressed in terms of wall shear stress, instead of wall shear rate. At each test temperature the rough/smooth transition occurred at a shear stress of about 10^5 Pa. The magnitude of τ_{cr} was established with an accuracy of $\pm 10\%$. Figure 10 shows the temperature dependence of Γ_{cr}, at $\tau = \tau_{cr}$. The data are here referred to the SDV system; however, more detailed results (to be discussed elsewhere) showed that τ_{cr} is nearly independent of die geometry or length.

At shear stresses greater than 120 kPa the extrudate surface was practically smooth.

Flow stability of AF05H

A gel constituted by 12% (w/w) gelatinized maize starch in water was tested at 60 °C by a "Couette" viscometer mod. Haake VT500. Figure 11 shows the viscosity and torque curves for two consecutive runs.

The viscosity curves of a virgin AF05H and of the same grade recycled three times by a twin screw extruder, are also compared in Fig. 12.

Wall-slip check for AF05H

Five abrupt entry capillaries with the same length-to-diameter ratio $L/D = 20$ and with different orifice dimensions (Table 2) were employed. AF05H melt was driven through the capillaries by a small gear pump mod. Maag Extrex at two temperatures, 140° and 150 °C. Figures 13 and 14 show the dependence of capillary radius on apparent shear rate at constant shear stress (Mooney, 1931).

Film blowing and mechanical testing

LDPE and AF05H film blowing studies were conducted with a $D = 40$ mm, $L/D = 25$ extruder fitted with a 100 mm semi-rotating spiral die. The extruder

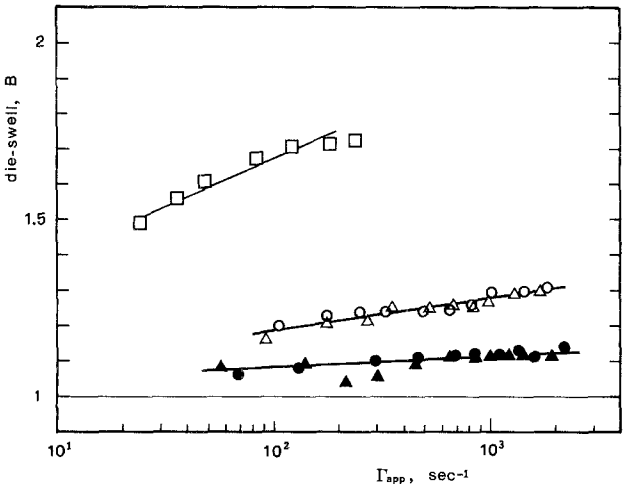

Fig. 9. Frozen (open symbols) and photographic die-swell (closed symbols) vs. apparent shear rate. a) □: LDPE at 180 °C; b) AF05H: ○, ● = 140 °C, △, ▲ = 150 °C

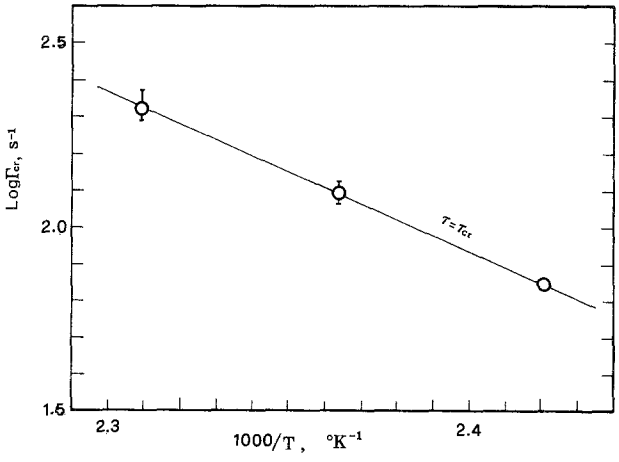

Fig. 10. The temperature effect on critical shear rate Γ_{cr} at the rough/smooth transition

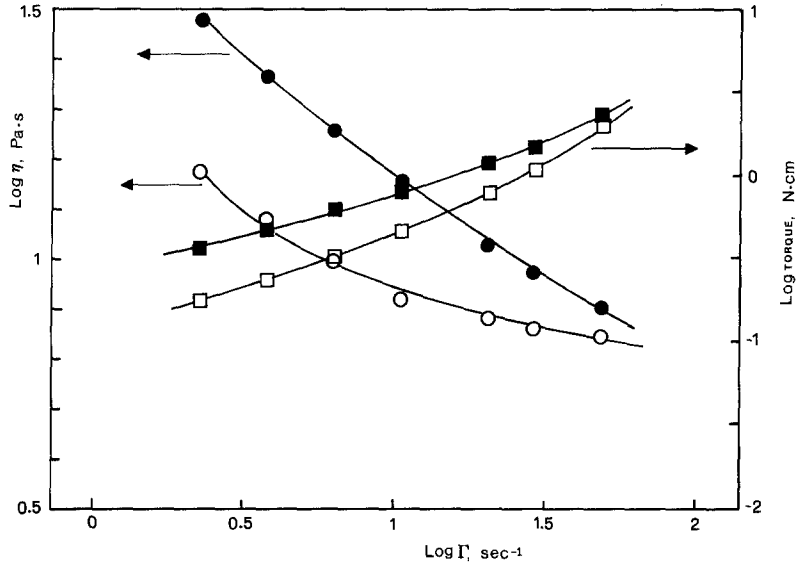

Fig. 11. "Couette" data for a 12% starch suspension in water (w/w) at $T = 60\,°C$. a) First experimental run (open symbols); b) Second run of the same sample (closed symbols)

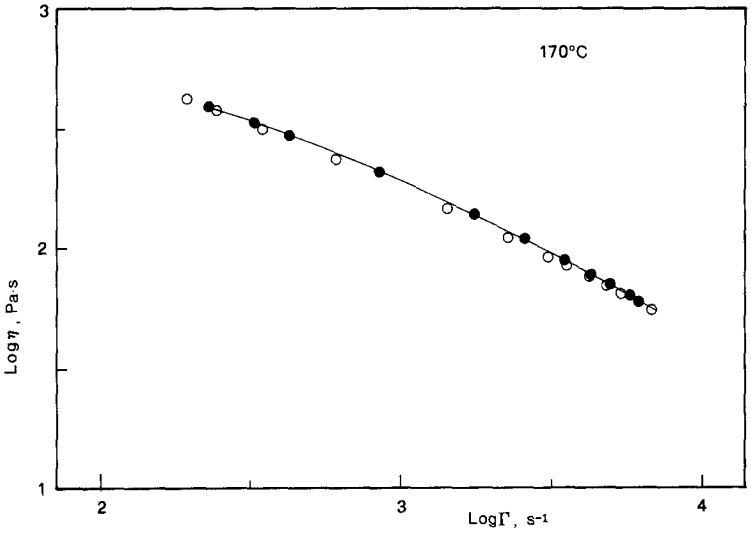

Fig. 12. Viscosity curves at $T = 170\,°C$ of: a) virgin AF05H (closed symbols); b) threefold recycled one (open symbols)

Table 2. Rheometric systems used in this work

Equipment	Sensor geometry	Feed system	Abbreviation	Purpose
Goettfert Rheograph 2002	L/D = 20, D = 1 mm	Reservoir + piston at constant speed	CAP 1	Low shear rate data for AF05H
Instron 3250 rheogoniometer	Cone & plate D = 20 mm, 6°		C&P	Low shear rate data for LDPE
Haake Fisons rheocord 90	Slit die visc. L × W × H = 140 × 20 × 1 mm	Single screw extruder D = 19 mm	SDV	Medium shear rate + exit press data for both polymers
Haake Fisons rheocord 90	L/D = 15, 20, 30 D = 1.27 mm	Single screw extruder D = 19 mm	CAP 2	High shear data for AF05H
Haake Fisons rheocord 90	L/D = 4, D = 2 mm	Single screw extruder D = 19 mm	CAP 3	Die-swell data for both polymers
Maag Gear pump	L/D = 20 D = 2.5, 2, 1.6, 1.25, 1 mm	Single screw extruder D = 19 mm		Wall-slip tests for AF05H at low rates

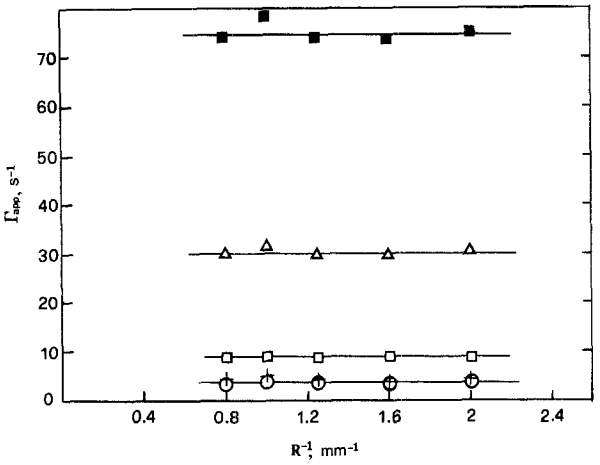

Fig. 13. Wall-slip tests for AF05H at 140 °C and different shear stresses: ○ = 22.8 kPa, + = 26 kPa, □ = 40 kPa, △ = 80 kPa, ■ = 120 kPa

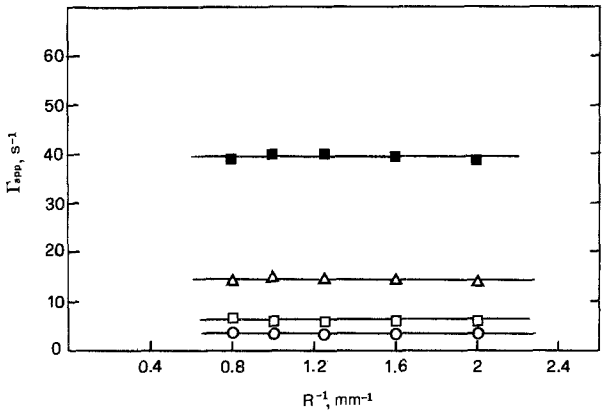

Fig. 14. Wall-slip tests for AF05H at 150 °C and different shear stresses: ○ = 17 kPa, □ = 21 kPa, △ = 35 kPa, ■ = 66 kPa

was equipped with a 3:1 compression ratio constant tapered screw. The die geometry and operating conditions are reported in Table 3. For AF05H, the wall shear stress applied at the die-land was approximately 180 kPa.

Blown film samples 30 μm thick, 50 × 10 mm length × width, were cut along the machine direction and tested by an Instron-4502 tensile machine according to ASTM-D 882 method. The mechanical properties of both the polymers are summarized in Table 4.

Discussion

At wall shear rates Γ higher than $10\,s^{-1}$, AF05H shows a sharp pseudoplastic behavior (Fig. 3); the relationship between viscosity and shear rate can be well described as a power law over a wide range of shear rates:

$$\eta = K \cdot \Gamma^{(n-1)} \quad \text{at } \Gamma > 10\,s^{-1}\,, \tag{7}$$

where: K = consistency ($Pa \cdot s^n$) and $n = 0.4 \pm 0.05$ in this work. The rheological data of Figs. 3 and 5 denote a highly structured melt: a yield stress $\tau_y \simeq 10^4$ Pa occurs, in fact, at low rates.

The experimental results of Fig. 5 show that the yield stress τ_y depends very little on temperature, but it becomes more detectable at higher shear rates as the temperature is increased.

The data of Figs. 13 and 14 demonstrate that the apparent shear rate, at low stresses, is independent of capillary radius; consequently, the polymer/wall adhesion exceeds τ_y in the flow region.

The flow activation energy E_τ of AF05H is approximately 10.2 Kcal/gmol; furthermore, there is no

Table 3. Die geometry and film-blowing conditions

Die diameter	100.0 mm	Draw ratio	7.7
Die opening	0.7 mm	Blow up ratio	3.0
Length of land	26.6 mm	Mass flow rate, kg/h	20.0
Film thickness	30.0 μm		
Die temperature °C	AF05H = 145 °C, LDPE = 160 °C		

Table 4. Mechanical properties of Mater-Bi® AF05H and LDPE riblene blown film (test method: ASTM-D882)

	Tensile stress at break (MPa)	Elongation at break (%)	Young modulus (MPa)	TEB* (MJ/m^3)
AF05H	18.3	408	113	44.7
LDPE	20.4	374	171	61.7

* Tensile energy to break.

evidence of shear stress effect on E_τ at $\tau \gg \tau_y$ (Fig. 4). The same value of activation energy holds at the rough/smooth transition ($E_\tau = E_\tau|_{\tau = 10 \cdot \tau y}$, Fig. 10).

The AF05H plot of normal stress N_{11}, against shear rate Γ shows that at a given temperature a power law relationship holds (Fig. 5).

$$N_{11}|_{ex} = \alpha \cdot \Gamma^{\beta} \quad , \tag{8}$$

where α and β are material constants.

For the range investigated here, a power law relation also holds between P_{ex} and shear stress τ. This behavior is in line with many literature data related to common thermoplastics (Han, 1971; Chan et al., 1990).

On the other hand, the large ratio N_{11}/τ for AF05H, even at low rates, allowed one to expect remarkable elastic effects at the die outlet (Bagley, 1970; Tanner, 1970). On the contrary, a negligible swelling near the die exit (photographic die-swell), and a slightly greater extrudate diameter at 30 mm far from it (frozen die-swell) are shown by Fig. 9. Moreover, the well known "melt fracture" phenomenon has not been observed here, not even at $\tau >$ 300 kPa.

The low die-swell values are in line with those of a recent experimental work (Mancuso, 1990) performed on AF05H. The swelling ratio of AF05H is a weak function of shear rate and seems to be temperature independent, at least for the range investigated here.

From the point of view of traditional polymers, a yield stress occurs either when there are strong interactions among droplets at low shear rates or when a polymer blend has an "interlocked" morphology (Han, 1981). Elastomer-modified thermoplastics at high rubber loading (Zosel, 1972; Han and Yang, 1987) and polymer melts highly filled with small rigid particles (Vinogradov et al., 1972; Wang and Lee, 1987) constitute further significant examples.

More recent experimental works (Bastioli et al., 1991a; Cangialosi, 1990) showed yield stresses τ_y of about 10^4 Pa for an experimental starch-based polymer (Bastioli et al., 1990).

Yield stress in gelatinized starch has also been observed and can be explained on the basis of aggregation or network forming reactions where individual molecules become interconnected at several points as a result of hydrogen bonds and physical entanglements (Remsen and Clark, 1978). The yield behavior of a gelatinized maize starch gel is also shown in Fig. 11.

In AF05H, maize starch is able to interact with ethylene vinylalcohol copolymer (EVOH) by means of both hydrophobic and hydrophylic interactions. A model has already been proposed (Bastioli et al., 1991b) considering large individual amylopectine molecules, interconnected at several points per molecule, as a result of hydrogen bonds and entanglements, by chains of amylose/EVOH complexes (Bastioli et al., 1993b). Figure 12 suggests that such interactions stabilize the flow properties of the polymeric system. Conversely, as shown by Fig. 11, consecutive shearing tests of a starch gel give different flow properties, revealing structure evolutions.

As a demonstration of the role played by hydrophobic interactions, AF05H does not dissolve in hot water under stirring, and generates spheres or sphere aggregates lower than 1 μm, generally 0.2 μm, with an unchanged starch/EVOH ratio (Fig. 15).

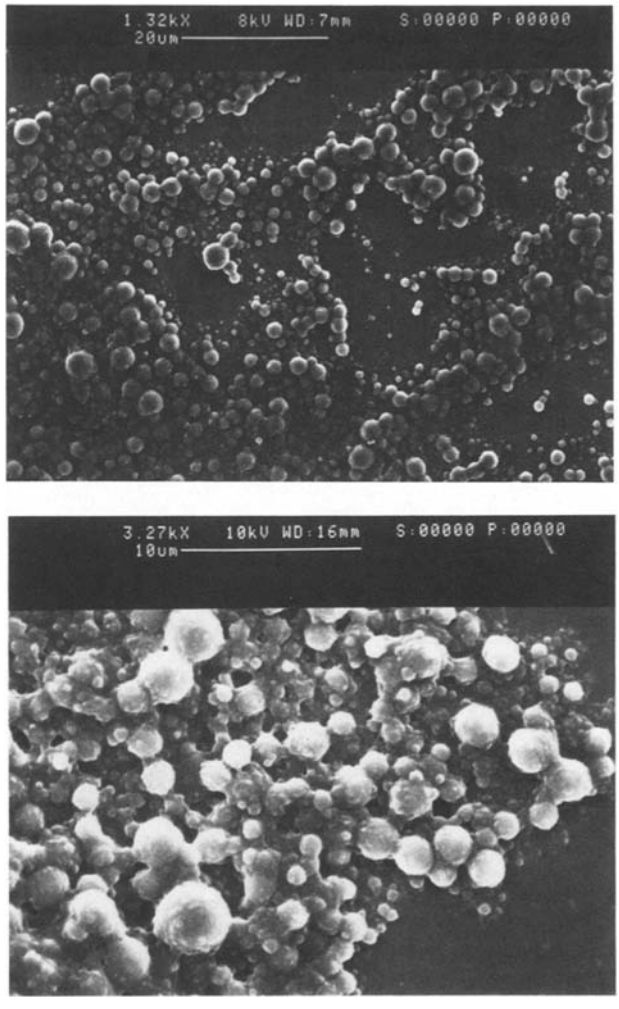

Fig. 15. Scanning electron micrographs of a AF05H film after boiling and ultrasonication. Scale bar is 20 μm for the upper and 10 μm for the lower micrograph

The presence of droplets which can interact by means of hydrogen bonds, producing a gel-like structural skeleton, explains both the observed yield phenomenon and the very limited die-swell. Furthermore, the temperature-independent die-swell of AF05H (Fig. 9) suggests that the generation of an interlocked structure is the governing mechanism. On the other hand, when hydrophobic interactions are strongly depressed, e.g., in amylopectine/EVOH systems, the extrudates do not show a droplet-like structure (Bastioli et al., 1993a) and high swelling ratios are observed.

In spite of its peculiar rheological characteristics the AF05H melt was easily film blown. Particularly, it showed a wide range of blow up ratio and high bubble stability; the latter is certainly due to its melt (tensile) strength, higher than that of LDPE at 210 °C (Mancuso, 1990). It is furthermore worth noting that the optimal film-blowing conditions here used for AF05H, and specifically a shear stress τ of about 180 kPa, generate in traditional plastics the well known "melt fracture" phenomenon (Bialas and White, 1969; Vlachopoulos and Lidorikis, 1971; Tadmor and Gogos, 1979).

As shown in Table 4, the tensile properties of AF05H and LDPE films are comparable in terms of strength and deformation, while LDPE is the more rigid and tough.

The rough/smooth transition detected on the surface of AF05H extrudate occurs at wall shear stresses lower than a critical value $\tau_{cr} \simeq 10 \cdot \tau_y$. Vinogradov et al. (1972) observed a similar surface instability for a carbon black filled polyisobutylene whose rough/smooth transition occurred at $\tau_{cr} \geq 10^2 \cdot \tau_y$. From a practical point of view, when the surface quality becomes important, the critical stress threshold can be thought of as the lower limiting condition for the extrusion process.

Conclusions

AF05H film blowing grade belonging to Mater-Bi® starch-based biodegradable polymers was considered. A general study of shear flow characteristics was performed at two typical processing temperatures, $T = 140$ and 150 °C. A strong pseudoplastic behavior at high shear stresses as well as yield stress at lower ones was detected.

The yield point of AF05H depends very little on temperature, but it appears more detectable at higher temperatures. After passing through the yield point, melt properties are dominated by a highly viscous flow. The non-linear Bingham fluid model can well describe its viscous behavior over a wide range of shear rates,

$$\tau = \tau_y + K \cdot \Gamma^n \quad \text{for } \tau > \tau_y$$
(K and $n < 1$ are constants) (9)

High levels of melt elasticity were detected from steady shearing tests, whereas its recoverable fraction was almost negligible, at least over a reasonable time scale.

The peculiar viscous and elastic behavior can be explained on the basis of a droplet-like morphology shown by AF05H, due to the ability of maize starch to generate also hydrophobic interactions with ethylene vinylalcohol copolymers (EVOH).

Although the rheological behavior of AF05H is far from being completely understood, the traditional shaping techniques and, particularly, the film blowing process can be easily performed. At room conditions, the tensile properties of AF05H blown film resemble those of low density polyethylene.

Acknowledgements

The authors are indebted to Professors G. Titomanlio (University of Salerno, Italy) and F. P. La Mantia (University of Palermo, Italy) for their scientific collaboration on Mater-Bi® products.

References

Bagley EB (1957) End corrections in the capillary flow of polyethylene. J Appl Phys 28:624–627

Bagley EB, Duffey HJ (1970) Recoverable shear strain and the barus effect in polymer extrusion. Trans Soc Rheol 14:545–553

Bastioli C, Bellotti V, Del Giudice L, Del Tredici G, Lombi R, Rallis A (1990) Biodegradable articles based on starch and process for producing them. Int Patent WO 90/10671

Bastioli C, Rallis A, Cangialosi F, La Mantia FP, Titomanlio G, Piccarolo S (1991a) Rheology, processing and mechanical properties of a starch based polymer. Presented at the European regional meeting of the polymer processing society, Sept 15–18, Palermo, Italy

Bastioli C, Bellotti V, Gilli G, Rallis A (1991b) Mater-Bi (starch based materials): properties and biodegradability. Presented at the international workshop on plastics waste management, December 9–12, New Orleans, LA

Bastioli C, Bellotti V, Del Giudice L, Gilli G (1993a) Mater-Bi properties & biodegradability. J Environ Polym Degr 1:181–191

Bastioli C, Bellotti V, Camia M, Del Giudice L, Rallis A (1993b) Starch/vinyl-alcohol copolymer interactions. Presented at the 3rd international scientific workshop on biodegradable plastics and polymers, November 9–11, Osaka (Japan)

Bialas GA, White JL (1969) Extrusion of polymer melts and melt flow instabilities. Rubber Chem Tech 42:682 – 690
Cangialosi F (1990) Caratterizzazione reologica e lavorabilità di miscele polimeriche a base di amido per film blowing. Chem Eng Thesis, Univ of Palermo, Italy
Chan TW, Pan B, Yuan H (1990) An experimental study of exit pressures for polymer melts. Rheol Acta 29:60 – 70
Han CD (1971) The effect of temperature on the elastic properties of polymer melts. Polym Eng Sci 11:205 – 210
Han CD (1976) Rheology in polymer processing. Academic Press, NY
Han CD (1981) Multiphase flow in polymer processing. Academic Press, NY
Han CD, Yang HH (1987) Rheological behavior of blends of PMMA and ABS. J Appl Polym Sci 33:1221 – 1229
Mancuso G (1990) Caratterizzazione reologica e lavorabilità di sistemi polimerici a base di amido per filmatura. Chem Eng Thesis, Univ of Palermo, Italy
Mooney M (1931) Explicit formulas for slip and fluidity. J Rheol 2:210 – 222
Remsen CH, Clark JP (1978) A viscosity model for a cooking dough. J Food Process Eng 2:39 – 64
Ryle TR (1991) Extruding degradable materials. Presented at the INDA conference, Oct 24 – 25, DC (USA)
Tadmor Z, Gogos CG (1979) Principles of polymer processing. Wiley, NY
Tanner RI (1970) A theory of die-swell. J Polym Sci 8:2067 – 2078
Vinogradov GV, Malkin AY, Plotnikova EP, Sabsai OY, Nikolayeva NE (1972) Viscoelastic properties of filled polymers. Int J Polym Mater 2:1 – 27
Vlachopoulos J, Lidorikis S (1971) Melt fracture of polystyrene. Polym Eng Sci 11:1 – 5
Wang KJ, Lee LJ (1987) Rheological and extrusion behavior of dispersed multiphase polymeric systems. J Appl Polym Sci 33:431 – 453
Zosel A (1972) Viscoelastic behavior of ABS polymers. Rheol Acta 11:229 – 237

(Received March 16, 1994;
in revised form May 15, 1994)

Correspondence to:

Dr. Angelos Rallis
Novamont spa (Montedison Group)
Via Fauser 8, I-28100 Novara (Italy)